

유연한 3D 열가소성 폴리우레탄 기반 폴리피롤-산화구리/이산화망간 복합체 슈퍼커패시터 제작에 관한 연구

조영희 · 사마야난 셀팜[†] · 임진형[†]

공주대학교 공과대학 신소재공학부

(2023년 11월 23일 접수, 2024년 1월 31일 수정, 2024년 2월 6일 채택)

Assembly of Flexible 3D Printed SCs from Thermoplastic Polyurethane Embedded Polypyrrole-CuO/MnO₂ Composites

Young Hwi Jo, Samayanan Selvam[†], and Jin-Heong Yim[†]

Division of Advanced Materials Engineering, Kongju National University, Budaedong 275, Seobuk-gu, Cheonan-si, Chungnam 31080, Korea

(Received November 23, 2023; Revised January 31, 2024; Accepted February 6, 2024)

초록: 유연한 3D 전극은 슈퍼커패시터와 배터리에 우수한 특성을 보이며 에너지 충전 시스템 분야에서 유망한 기술로 주목받고 있다. 그러나 유연성으로 인한 느린 전자 이동속도, 질량 증가, 그리고 낮은 에너지 밀도가 단점으로 꼽힌다. 이러한 우려를 효과적으로 해결하기 위해, 3D 열가소성 폴리우레탄(3D TPU)-폴리피롤(PPy)-CuO/MnO₂ 하이브리드 슈퍼커패시터 전극(3D TPU-PPy-CuO/MnO₂)을 제조하였다. TPU-PPy-CuO/MnO₂ 전극은 약 10000 회의 주기 동안 98.8%의 주기 안정성을 유지하며 88 mFcm⁻²의 용량 성능을 보였다. 이 3D 전극의 우수한 전기화학적 특성은 특별한 복합 형태에서 기인하는데, 이는 높은 전도성, 빠른 전자 이동, 짧은 이온 확산 거리, 그리고 향상된 전기화학적 성능을 가능하게 한다. 이러한 결과는 슈퍼커패시터 전극 소재의 구조적 엔지니어링에 대한 간단하고 효과적인 방법을 강조하며, 보다 지속 가능하고 확장 가능한 3D 하이브리드 에너지 시스템의 창조를 가속화할 것으로 기대된다.

Abstract: Flexible 3D electrodes are showing promise in the arena of energy packing systems since they combine the best features of supercapacitors (SCs) and batteries. But its limited potential is a result of flexibility, slow electron transfer, mass loading, and insufficient energy density. To effectively address these concerns, a three-dimensional thermoplastic polyurethane (3D TPU) embedded-polypyrrole (PPy)-CuO/MnO₂ hybrid SC electrode (3D TPU-PPy-CuO/MnO₂) is proposed for 3D SCs. The TPU-PPy-CuO/MnO₂ electrode has a remarkable cyclic stability of 98.8% even after 10000 cycles, allowing it to reach the capacitance performance of 88 mFcm⁻². The 3D electrode's outstanding electrochemical property may be traced back to its peculiar composite morphology, which plays a critical role in enabling high conductivity, rapid electron transfer, short ion diffusion distance, and superior active sites for improved electrochemical performance. These findings highlight a simple and effective method for structurally engineering the active SC electrode material, which should speed up the creation of more sustainable and scalable 3D hybrid energy systems.

Keywords: 3D printing, thermoplastic polyurethane, polypyrrole, flexible electrodes, 3D supercapacitors, vapor phase polymerization, polymer metal-oxides matrix.

Introduction

The demand for energy storage units and reworking that are both economical and favorable to the environment has sig-

nificantly increased, and smart devices that integrate both energy conversion and storage have attracted increasing attention as a major breakthrough for efficient energy usage.^{1,2} Many attempts and reports have examined and manufactured hybrid supercapacitors (SC) electrodes using unique methods, for example, stem coating, 3D dual extrusion, microextrusion, etc.³⁻⁶ These methods are expensive or can't process all the materials needed to make polymer composite SC electrodes. To create functional

[†]To whom correspondence should be addressed.
jhyim@kongju.ac.kr, ORCID[®] 0000-0002-3557-9564
sselvam222@gmail.com, ORCID[®] 0000-0003-3227-1158
©2024 The Polymer Society of Korea. All rights reserved.

SCs, various techniques were needed. Additive engineering 3D printers can construct practically several geometrically complicated outline and pattern cutting-edge materials with exact conformal depositions.⁷⁻⁹ It has been used to develop flexible SCs, but it is still difficult to attain good and stable performance, especially under mechanical bending.^{10,11} Other benefits of this technology include making complicated SCs, flexible packaging due to 3D forms, and commercial consumer 3D electronic fabrications.

In terms of thermoplastic polyurethane (TPU) matrix for 3D production of TPU-constructed flexible electrodes, it appears easy to achieve polymer hybrid coatings, efficient structures, and strategies by merging the bendable TPU constructed filaments with particular category of exceedingly conductive filler, for example, carbon nanotubes (CNT) or silver nanowires. This can be done by combining the highly conductive filler with the exceedingly elastic TPU substantial filaments.¹²⁻¹⁴

However, the technical challenge is that inappropriate and excessive additions can quickly lead to well hard TPU matrix filaments for SC electrode material coating. This is a result of the fact that TPU matrix composite filaments are made of thermoplastic polyurethane. Additionally, the dispersion of conductive sources in the TPU layer also has a direct influence on the mechanical and electrochemical capabilities of the 3D SCs.^{15,16} Therefore, it is stated that the precondition for achieving good performance capabilities is both advanced operational flexibility and improved material regularity for 3D printing of TPU matrix composites. This is because of how flexible the structure is for SCs. As a potential method for improving the materials that are used to store and conduct energy, polypyrrole (PPy) has been given a lot of consideration as a prospective component in the development of SCs. This is as a result of their remarkably extraordinary power density, increased lifespan, express charging and discharging capabilities, and great possibilities for adoption in a variety of industries, including the automotive and aerospace industries.

In recent years, there has been an uptick in research and development efforts directed toward the production of energy storage and sensors and dependable nitrite sensors through the utilization of a wide variety of nanocomposite materials, including those that are based on PPy. SCs electrode materials composition with current directing polymer matrixes or nanomaterials (metal oxides), as a result of the faradaic charge storage, pseudocapacitors always have larger specific capacitances than the electrical double-layer capacitors.¹⁷⁻¹⁹ As of their extraordinary specific capacitances, transition metal oxides perhaps MnO_2 ,

CuO , V_2O_5 , WO_3 , etc.¹⁸⁻²² are interesting active electrode materials for the use of SCs. Specifically, MnO_2 has a potential specific capacitance, is cheap, and is easily available.

In order to improve conductivity, specific capacitance, mechanical stability, and flexibility, linking conducting polymers through MnO_2 was found to be a good technique. The MnO_2/PPy composite is commonly used in the fabrication of SCs because of PPy's high conductivity, strong environmental stability, and ease of synthesis.²³ While CuO shows promise as a high-capacity electrode,²⁴ it still faces obstacles such as low experimental specific capacitance, poor conductivity, and cycling stability. Many studies have focused on modifying CuO through compositing with other transition metal oxides in an effort to find solutions to the aforementioned issues. In our previous reports, we developed 3D TPU/PPy for strain sensor applications and evaluated the performance of PPy through the vapor phase polymerization (VPP) process.^{25,26}

From the aforementioned observations and views, the present work focused its attention on the intention technique of elastic formations, the progression assurance for structural constructions, fabrications route, and the electrical-mechanical comportment of 3D TPU matrix as flex-SCs that were studied from fabricated 3D printing matrixes. The 3D-printed TPU matrix composite substrates were designed for periodic geometries, and their substrates were incorporated with PPy under VPP on TPU film. According to the electrical-mechanical experiments, with the assistance of PPy-CuO/ MnO_2 matrixes for high-performance SCs.

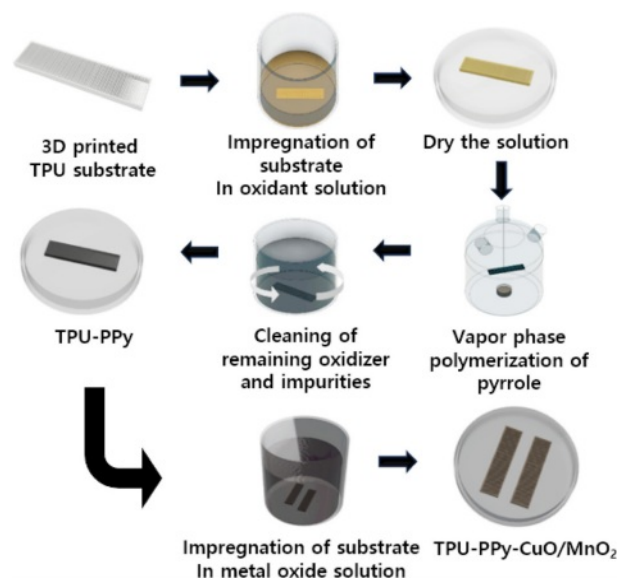


Figure 1. Schematic representation of 3D-produced TPU, TPU-PPy, and TPU-PPy-CuO/ MnO_2 composites.

Experimental

Materials and Reagents. The substrate used for the 3D fabrication process was a TPU foundation (eSUN, eTPU-95A, breadth 1.75 mm, China). During oxidative polymerization, ethanol (Samchun Pure Chemical, Korea) was utilized as the solvent for the oxidizing mediator, iron(III) *p*-toluenesulfonate (FTS, Sigma-Aldrich, USA). The conductive polymer PPy monomer utilized for the oxidative polymerization was pyrrole (ACROSE, GEEL, Belgium). To improve the SC's chemical and electrical performance, additional additives such as copper oxide and manganese dioxide were added. Metal oxides were adsorbed on the substrate surface using ethylene glycol (Samchun Pure Chemical, Korea).

Fabrication of 3D TPU, TPU-PPy, and TPU-PPy-CuO/MnO₂. 3D printer (ROKIT, AEP II, Korea), was utilized to assemble TPU. Flexible TPU was 3D printed with a substrate angle of 0 degrees and a 70% infill density. After being soaked in ethanol containing an oxidizing agent at a concentration of 30 weight percent (wt%) for 30 minutes, the TPU was agitated for about 10 minutes. The finished product was allowed to air dry at room temperature for 60 minutes. After adding FTS to the TPU, the mixture was placed in a polymerization room, where PPy was polymerized for 6 hours in a nitrogen atmosphere. The resultant TPU-PPy was air-dried for a minimum of 12 hours after being rinsed in ethanol for 20 minutes to eliminate any residual oxidizing agents.²⁷

The TPU-PPy-CuO/MnO₂-PPy-CuO/MnO₂ made by mixing 0.02 g CuO, 0.02 g MnO₂, and 15 mL of ethylene glycol for 10 minutes while stirring at 1200 rpm. Then, we added 35 mL of DI water and sonicated the mixture at 50 °C up to 90 minutes. The TPU-PPy composite was mixed with the dispersion solution, then subjected to a 6-hour reaction in an oil bath at 60 °C, followed by 12-hours of drying in an oven at the same temperature. Figure 1 shows the preparation procedures for TPU-PPy-CuO/MnO₂ composites.

Testing and Analyzing Characteristics. The Fourier transform infrared spectrometer (FTIR, PerkinElmer, USA) and field emission scanning electron microscopy (FE-SEM, TESCAN, Česko) were operated to analyze the morphology of the matrixes. Universal testing machine (UTM, Hounsfield, H10KS, USA) to check the physical property analysis. Electrochemical impedance spectroscopy (EIS) measurements of the SC's performance were taken exhausting a Workstation (SP-150, Biologic, France) and a 6M KOH alkaline electrolyte.

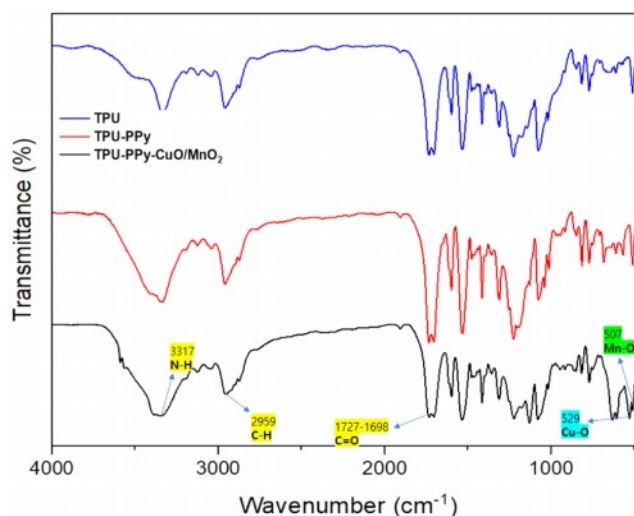


Figure 2. FTIR studies data for (a) TPU; (b) TPU-PPy; (c) TPU-PPy-CuO/MnO₂ composites.

Results and Discussion

FTIR studies of 3D TPU-PPy and TPU-PPy-CuO/MnO₂. In order to study the chemical composition and interaction between TPU, TPU-PPy, and TPU-PPy-CuO/MnO₂ in 3D matrixes, as well as to determine the impact of processing VPP technique and material composition on the 3D composite, FTIR analysis was carried out (Figure 2). The peak around 3400 cm⁻¹ for clean 3D TPU is explained by the stretching of hydrogen bonds (Figure 2(a)). Aliphatic CH₂ exhibits symmetric and asymmetric axial deformation, respectively, as indicated by the bands at 2904 and 2917 cm⁻¹.²⁸ The 1730 cm⁻¹ point is also related to free carbonyl stretching vibration; however, the 1707 cm⁻¹ band is accompanied by carbonyl groups that are hydrogen bound. The FTIR of TPU-PPy (Figure 2(b)), the unique engagement peaks of C-OH promises on the external of TPU were linked to the strong extending vibration peaks seen at 1120 cm⁻¹ and 1137 cm⁻¹ notations a and b, respectively. The C-N stretching, N-H bending, and aliphatic C-O stretching are accompanied by peaks at 1970, 1527, 1306, and 1220 cm⁻¹, respectively.²⁹

After polymerization and metal oxide coating, the FTIR results show (Figure 2(c)) that the N-H peaks that were previously attributable to TPU and PPy, which ranged in frequency from 2959 to 3317 cm⁻¹, widened significantly because PPy was present. In addition, the peaks corresponding to the metal oxides (CuO, MnO₂) that were studied in this experiment were seen at 529 cm⁻¹ (Cu-O) and 507 cm⁻¹ (Mn-O) peaks.^{30,31}

Morphological Analysis TPU-PPy-CuO/MnO₂ Composites.

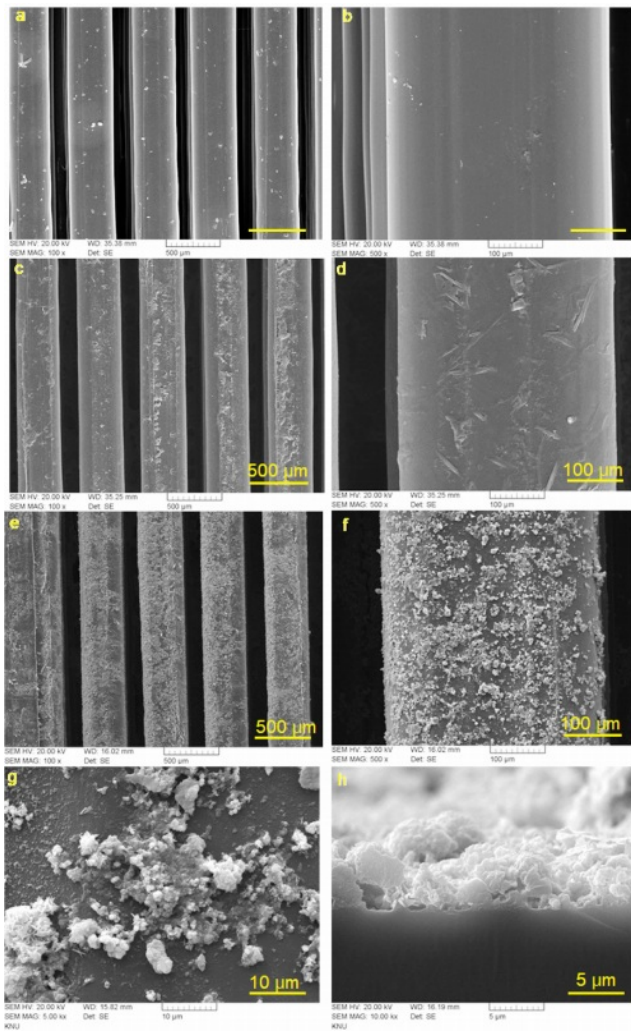


Figure 3. SEM analysis of 3D (a, b) TPU; (b, c) TPU-PPy; (e, f, g) TPU-PPy-CuO/MnO₂ composite surface; (h) cross-section of TPU-PPy-CuO/MnO₂.

3D-printed TPU, TPU-PPy, and TPU-PPy-CuO/MnO₂ combinations were evaluated by TESCAN-MIRA 2- FE-SEM and compared in Figure 3. The 3D-printed TPU surface clearly shows the filmy surface (Figure 3(a) and (b)), and the TPU-PPy sample surface contains particles of PPy with a dependable size and distribution all over the TPU matrix (Figure 3(c) and (d)). Figures 3(e) and f show that for the TPU-PPy-CuO/MnO₂, the composites showed compact block morphologies independent of the residence period for the first step of PPy via VPP. The tiny cores were coated with polymers with short chains because the oxidant (FTS) to monomer ratio was high. As a result of their small size and high specific area, the TPU-PPy-CuO/MnO₂ composite particles tended to agglomerate, lowering the surface energy.

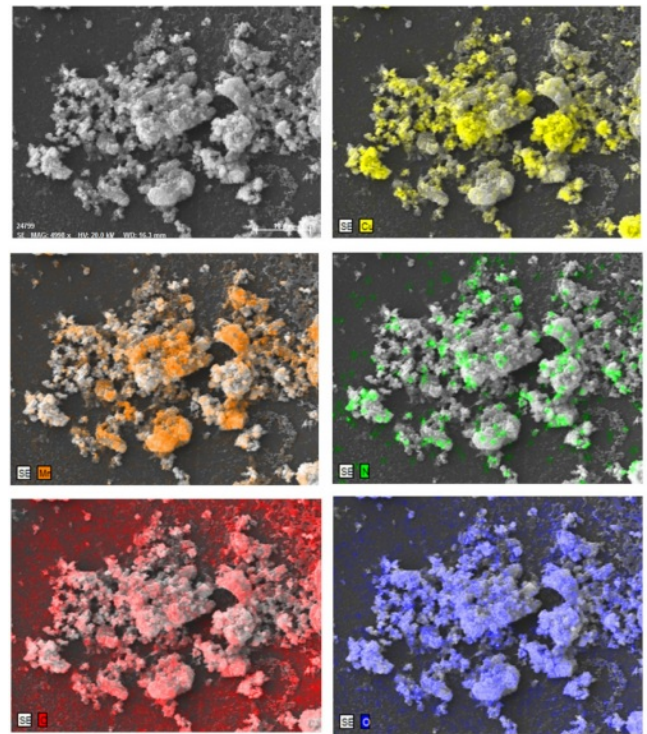


Figure 4. EDS mapping of the analysis TPU-PPy-CuO/MnO₂ composite.

As demonstrated in the SEM of TPU-PPy and TPU-PPy-CuO/MnO₂, the combined morphology changed from amorphous blocks to aggregated spheres (PPy), metal oxide needles (CuO), and flaks as the residence.

At high magnification, the cross-section surface clearly shows the morphological changes from metal oxide coatings (Figure 3(g) and (h)). From these surface results, the metal particle's crystal size grows as the lodging time for the initial major stage increases, which is the expected outcome. Additionally, particle aggregation was reduced due to the production of polymers by extensive chains caused by CuO and MnO₂ in the TPU-PPy-CuO/MnO₂ combination. Also, the EDS mapping (Figure 4) of composite clearly showed the important elements appearances (Cu, Mn, N, C and O), which are the confirmation of the composite formation.

Mechanical Possessions of 3D TPU-PPy and TPU-PPy-CuO/MnO₂. The mechanical actions of TPU-PPy and TPU-PPy-CuO/MnO₂ combinations are depicted in Figure 4 and can also be found in Table 1. The clean TPU matrix stress-strain curve makes it abundantly clear (Figure 5(a)), and the addition of TPU-PPy and TPU-PPy-CuO/MnO₂ causes a reduction in both the modulus and the strength of the material. The horizontal percentage was also influenced (Figure 5(b)). Table 1 also

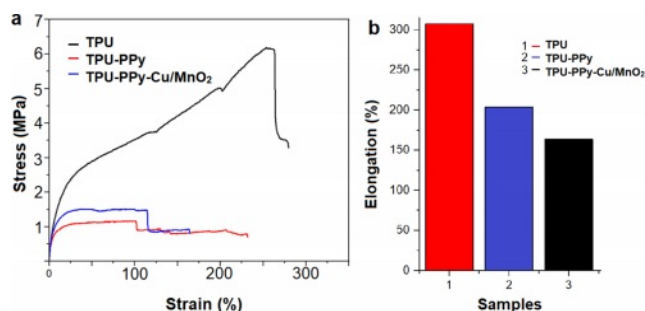


Figure 5. (a) Stress-strain curve; (b) horizontal percentage TPU, TPU-PPy, and TPU-PPy-CuO/MnO₂ composites.

Table 1. Stress-strain Curve of TPU, TPU-PPy, and TPU-PPy-CuO/MnO₂ Composites

Samples	Tensile Strength (Kg _f /mm ²)	Horizontal at break (Kg _f /mm ²)
TPU	0.26	4.05
TPU-PPy	0.43	3.67
TPU-PPy-CuO/MnO ₂	0.16	3.14

clearly indicates the tensile properties of the composites; the tensile strength is reduced from 0.26 Kg_f/mm² (TPU) to 0.16 Kg_f/mm² (TPU-PPy-CuO/MnO₂). Both the uniform dispersion of CuO and MnO₂ particles, which have stiff characteristics, and the uniform dispersion of PPy particles, which lend flexibility to the TPU matrix, can be credited with this result. The observed decline in mechanical characteristics can be recognized to a number of factors, including the weakening of intermolecular connections, changes in thermal, chemical, and structural properties brought on by oxidation, and the addition of heat brought on by CuO and MnO₂.

The infill patterns of 3D TPU also impact the mechanical characteristics of soft TPU, TPU-PPy, and TPU-PPy-CuO/MnO₂ composites that are 3D printed. The tensile stress appears to be distributed evenly all over the infill outline track for all 3D-printed matrixes when the material is stretched in their particular two directions. The structural lines, relative to the extending track, are able to resist the initial threshold of stretching of the infill shapes. Distinct square or pattern fillings with metal oxide coatings, the infill patterns of 3D TPU can be altered by adjusting or narrowing the original angle. This effect enables three infill patterns to withstand greater stress and strain for pure 3D TPU, and the metal oxide coatings are leading to increased durability. Conversely, lower stress and strain values were observed for the pure TPU patterns due to the stress being concentrated and layered on the two side edges. Also, VPP polymerizing PPy

through TPU also influenced the maximum stress and strain. Increased rigidity and stiffness can be achieved by crosslinking TPU with PPy and CuO/MnO₂ through hydrogen and van der Waal's bonding.³²

Electrical Characterizations of TPU-PPy and TPU-PPy-CuO/MnO₂ Constructed SCs. The electrochemical behaviors of the TPU-PPy and TPU-PPy-CuO/MnO₂ SC electrodes were examined from a workstation (SP-150, BioLogic). This instrument was employed to achieve the corresponding cyclic voltammetry (CV), galvanostatic charge-discharge (CD), and electrochemical impedance spectroscopy (EIS).

The fabrication of the SC electrode, which was accomplished through the use of a symmetric sandwich-type configuration, to provide further information, the sandwich-type system was used to create the composite film SC. electrolyte of the gel type, composed of 6 M KOH and PVA, was developed for use in flexible electrodes. Coating the electrolyte over a 3D printed electrode region of the film surface was accomplished through the use of the doctor-blade approach, which ensured equal dis-

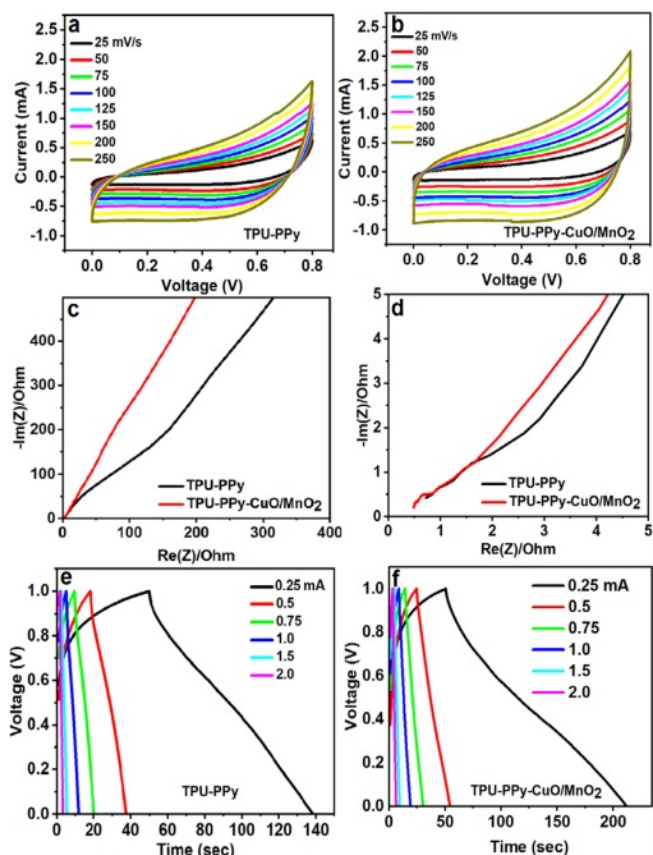


Figure 6. CV, EIS (low-high frequency regions), and GCD profiles of 3D printed: (a, c, e) TPU-PPy; (b, d, f) TPU-PPy-CuO/MnO₂ composites.

tribution. Additionally, filter paper (Whatman) was utilized as a separator. For additional insulation and to ensure that there was no leakage, the system that was manufactured was wrapped with safety tape (Scotch). Each and every one of the CV, CD, and EIS readings were carried out in a KOH electrolyte at the indicated scan rates.

Figure 6(a) and (b) display the CV illustrations of the TPU-PPy and TPU-PPy-CuO/MnO₂-based SCs that were obtained at a variety of scan rates. With regard to the symmetric devices, it was noted that the inclusive potential window sweeps contained redox peaks that were of significant significance. CV was used to test the composite film SCs, in which the voltage assortment was from 0 to 0.8 V and the scan rate was varied. Each and every one of the CV profiles that were carried out for the composite electrodes had the following scan rates: The scan rates of each CV curve are 25, 50, 75, 100, 125, 150, and 200 mV/s. The fact that the CV details were not symmetrical and contained two different collections of redox peaks provided evidence that the nature of the material was pseudo-capacitive. The TPU-PPy-CuO/MnO₂ SCs exhibit an increased area of CV curve when compared with TPU-PPy. It was determined that the agreeing typical redox peaks.

EIS was performed to recognize the charge transfer status and resistance in the TPU-PPy and TPU-PPy-CuO/MnO₂ SCs electrode/electrolyte boundaries and inner area. The Nyquist scheme is shown in Figures 5(c) and (d). The electrode materials' EIS curves show solution resistance (R_s), the frequency section in Figure 6(c), and an uncurving line superior above 45° to the actual axis (real) near the imaginary axis in the squat-frequency section (Figure 6(d)), demonstrating good capacitive behavior. The EIS line has fewer imaginary sections and is more vertical, suggesting low diffusion resistance (Warburg impedance, W).³³

Figure 6(e) and (f) depict the galvanostatic charge/discharge (GCD) data with corresponding current densities extending from 0.25 mA to 2.0 mA. These curves appear at different current densities. The trend of the CV curve was similar to the shape of all of the TPU-PPy and TPU-PPy-CuO/MnO₂ curves, which were triangular in shape and relatively symmetrical.

The galvanostatic charge-discharge (GCD) summaries of all composite SCs exhibit their typical curves at various current densities (0.25, 0.5, 0.75, 1.0, 1.5, and 2.0 mA). This evidently validates the characteristic pseudo-capacitance and electric double-layer capacitor behavior of the TPU-PPy-CuO/MnO₂ electrode materials. Moreover, the curves are straight and symmetrical. An extremely minute quantity of the typical internal

resistance was noticed in each and every discharge curve. This was due to the fact that the electrode materials were electrically connected to one another. By utilizing rapid surface adsorption-desorption reactions, electrode materials that possess a high electrical conductivity are able to progress electron charge transfer reactions at the interface. The galvanostatic discharge curves were employed to compute the specific capacitance, and eq. (4) was utilized to calculate the performances.³⁴

$$C = \frac{I\Delta t}{A\Delta V} \quad (1)$$

The abbreviations $I(A)$ indicate the current, $t(s)$ symbolizes the time for thorough discharge, $A(\text{cm}^2)$ represents the area of the dynamic electrode substantial, and V represents the voltage alteration afterward full charge or discharge. The obtained areal capacitances are shown in Figure 7(a). The specific capacitances

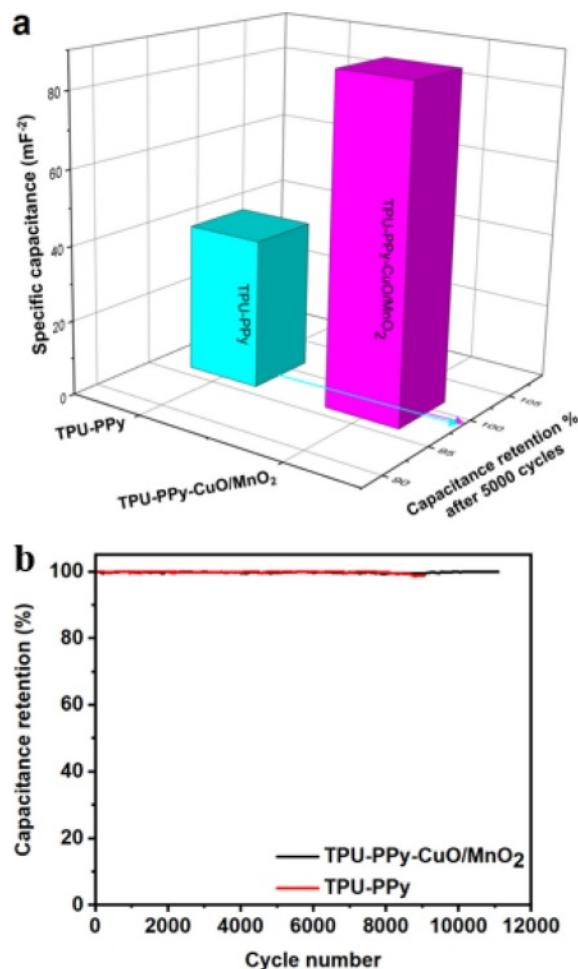


Figure 7. (a) 3D graph of specific capacitance with capacitance retention; (b) cyclic stability TPU-PPy and TPU-PPy-CuO/MnO₂ composites.

Table 2. Comparison of 3D TPU-PPy-CuO/MnO₂ with Other 3D Metal Oxide and Polymer SC Electrode with Recent Reports

3D SC electrodes	Spc, Capacitance	Cyclic stability (cycle)	Flexible conditions	Ref.
TPU-PPy-CuO/MnO ₂	88 mFcm ⁻²	12000	Horizontal Bending	This work
MXene-N@Zn-Co	7.8 F g ⁻¹	6000	NA	39
Porous Carbon printing	328 mFcm ⁻²	400	NA	40
graphene aerogel/MnO ₂	11.9 Fcm ⁻³	1000	NA	41
MXene@PTC*	30.2 mFcm ⁻²	10000	Bending only	42
Graphene/MoS _x	11.6 mFcm ⁻²	10000	NA	43

NA: No data available; *PTC: PLA/TPU/CB (polylactic acid/Thermoplastic polyurethane/ carbon black); MoS_x: molybdenum sulfide

of the combination electrodes have been estimated on the discharge curves. The specific capacitance of the TPU-PPy and TPU-PPy-CuO/MnO₂ 3D printed composite SCs was that the TPU-PPy performed with around 40 mFcm⁻² and 88 mFcm⁻² for the TPU-PPy-CuO/MnO₂. This is a significant improvement over the TPU-PPy-CuO/MnO₂ 3D SC, which is evidence of the effect on the polymerization process, and metal oxide coatings have good performance and considerable improvements after CuO/MnO₂ treatments.

Figure 7(b) shows that cyclic stability is another criterion for evaluating the performance of the SC. The 3D composite SCs made of TPU-PPy and TPU-PPy-CuO/MnO₂ were studied for their long-term cyclic performance more than 10000 cycles using GCD tests conducted. The two 3D SCs have substantially lower capacitance retention rates (~98.8%). This type of 3D flexible SC device for storing energy levels over a prolonged period of time would benefit from the stability and capacitance retention capabilities achieved. The composite electrode materials are likely responsible for the achieved cyclic stability. Merging 3D TPU with PPy and CuO/MnO₂ strengthens the bonds between the composite's constituent parts, leading to enhanced mechanical characteristics and capacitance cycle stability.^{35,36}

The fabricated 3D SC device was checked under different elongating and bending conditions to check in order to study the mechanical strength and flexibility (Figure 8). The obtained CV graph (Figure 8(a)) at both conditions revealed a slight difference in the redox conditions, and the EIS plot (Figure 8(b)) showed similar performance, which may be due to the ion transport delay under elongation or the electrode spore distance difference. This elongation and bending state are not permanent conditions; the flexibility or elasticity is continuously changing behavior. Also, the current variation, as previously checked SC area is 1 cm² and for the real-time SC for elongation studies, the SC area is 4 cm². Due to the large size of the SC the current and conductivity differences showed.

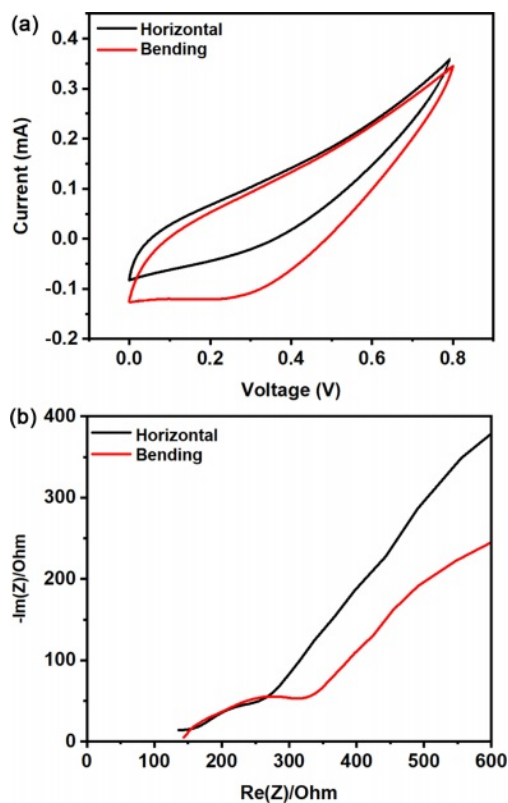


Figure 8. (a) CV; (b) EIS of TPU-PPy-CuO/MnO₂ SC performance under elongation and bending conditions.

The 3D printed SC performance was compared with recent reports in terms of 3D printed metal oxides and polymer composites (Table 2). From the comparison data, this reported 3D TPU-PPy-CuO/MnO₂ SC exhibited better cyclic stability and flexibility performances. Also, it clearly seems the bending and horizontal performances are very important, even with the high capacitance obtained. The PPy composed of 3D structural electrode surfaces; the preferred TPU-PPy-CuO/MnO₂ composite samples are abundant in carbon, oxygen, and nitrogen in a variety of charge-discharge states. Going along with the contradictory

trend as the -N+ component is the prospectively dependent -N = section of PPy. It is clear from these findings that the oxidation and reduction of PPy nitrogen are responsible for the charge-storage of the composite electrode in the TPU-PPy-CuO/MnO₂ hybrid system.

Hence, PPy can be intercalated between TPU and CuO/MnO₂ layers, increasing the distance between them and hence speeding up charge transfer in TPU-PPy- CuO/MnO₂ energy storage devices. Freestanding flexible electrodes based on TPU-PPy-CuO/MnO₂ were conceptualized as conductive polymer-based electrodes with much improved electrochemical performances through the intercalation of PPy into 3D TPU. The results demonstrate that the electrolyte penetration, diffusion, and mass transfer are all affected by the intercalation of PPy, which inhibits the restacking of metal oxides.. The PPy backbones are reinforced by the strong connections formed with the CuO/MnO₂ and TPU surfaces, which not only have good conductivity but also accurate charge-carrier transport pathways. Moreover, a standalone 3D TPU-PPy-CuO/MnO₂ supercapacitor with outstanding capacitance flexibility is built utilizing this composite.^{37,38} The proposed composite enabled electron transport and ionic diffusion in a three-dimensional (3D) network. In addition to CuO/MnO₂ stacking and PPy development, the 3D printed scaffolding improves the structural stability of the nanocomposite. The electrolyte that is adsorbed onto composite layers spontaneously might be thought of as an additional liquid "spacer" that allows for rapid ion diffusion kinetics.

The incorporation of thermoplastic urethane (TPU), which allows for mechanical flexibility in the design of energy storage electrodes, has also led to the development of a flexible supercapacitor. As an ultrafast electron transport layer, metal oxide decorated films are used on the electrodes of supercapacitors. The specific capacitance is evidently improved by the PPy layers, which also decrease internal resistance, increase the rate of electron transfer, and improve the transit rate of electrolyte ions in the diffusion layer. It is also possible to assess the cycle-life of PPy by using a layer of metal oxides, which have great mechanical properties, as a support material. The improved capacitance property of PPy is a result of its homogeneous thin layer presentation on TPU and metal oxide surfaces, which greatly improves electrode-electrolyte interaction. Moreover, PPy's aromatic rings would interact strongly with one another, considerably simplifying the charge-transfer process.^{44,46}

In addition, the capacitive characteristics can be improved for metal oxide-coated SCs because CuO/MnO₂ loading can lead to severe PPy and metal oxide agglomeration and restack-

ing, which includes the conductivity of the electrochemically active mass transport PPy and metal oxide network that allowed electrons to flow between the two materials, leading to PPy's significant capacitance contribution. In addition, the 3D-printed composite-based SC device had better capacitance and cycling stability due to the PPy and CuO/MnO₂ tight attachments to the 3D TPU sheets.

Conclusions

3D-printed flexible TPU-PPy-CuO/MnO₂ functionalized composites were used to successfully fabricate a 3D SC. The 3D-printed film electrode performed excellently in electromechanical and mechanical strength experiments. In terms of electromechanical SC performance, the 3D film electrode functioned excellently. With a specific capacitance of 88 mFcm⁻². The 3D-printed energy storage system was able to maintain its initial performance level (98%) even after 10000 cycles. Smart electronic and flexible 3D devices may one day make use of the combined flexible multifunctional energy storage system as a SC.

Acknowledgments: This research was supported by the National University Development Project by the Ministry of Education in 2023.

Conflict of Interest: The authors state that there is not at all conflict of interest.

References

1. Amir, M.; Deshmukh, G. R.; Khalid, M. H.; Said, Z.; Raza, A.; Muyeen, S. M.; Nizami, A. S.; Elavarasan, R. M.; Saidur, R.; Sopian, K. An Integrated Survey of Developments, Global Economical/environmental Effects, Optimal Scheduling Model, and Sustainable Adaption Policies. *J. Energy Storage* **2023**, *72*, 108694.
2. Shao, C.; Zhao, Y.; Qu, L.; Recent Advances in Highly Integrated Energy Conversion and Storage System. *SusMat.* **2022**, *2*, 142-160.
3. Mousavi, M. S.; Hashemi, A. S.; Kalashgri, M. Y.; Gholami, A.; Binazadeh, M.; Chiang, W. H.; Rahman, M. M. Recent Advances in Energy Storage with Graphene Oxide for SC Technology. *Sustainable Energy Fuels*, **2023**, *7*, 5176-5197.
4. Benoy, S. M.; Pandey, M.; Bhattacharjya, D.; Saikia, B. K; Recent Trends in SC-battery Hybrid Energy Storage Devices Based on Carbon Materials, *J. Energy Storage*, **2022**, *52*, 104938.
5. Khosrozadeh, A.; Singh, G.; Wang, Q.; Luo, G.; Xing, M. SC with Extraordinary Cycling Stability and High Rate from Nano-architected Polyaniline/graphene on Janus Nanofibrous Film

- with Shape Memory, *J. Mater. Chem. A*, **2018**, 6, 21064-21077.
6. Liu, J.; Ma, J.; Chen, J.; Sun, J.; Liu, C.; Liang, S.; Zou, L. Design and Simple Preparation of a Novel 1D/2D/3D Multi-structure Composite for High-performance SCs. *J. Alloys. Compd.* **2023**, 963, 171034.
 7. Yang, G.; Zhou, J.; Zhang, Z.; Song, Y.; Li, Wei.; Chen, Z.; Chu, W.; Chen, J.; Xue, Y.; Peng, C.; Tang, W. Engineering 3D Vertically-aligned Lamellar-structured Graphene Incorporated with Polypyrrole for Thickness-independent Zinc-ion Hybrid SC. *J. Alloys. Compd.* **2023**, 938, 168447.
 8. Areir, M.; Xu, Y.; Harrison, D.; Fyson, J. 3D Printing of Highly Flexible SC Designed for Wearable Energy Storage, *Mater. Sci. Eng. B*, **2017**, 226, 29-38.
 9. Godoi, F. C.; Prakash, S.; Bhandari, B. R. 3D Printing Technologies Applied for Food Design: Status and Prospects *J. Food Eng.* **2016**, 179, 44-54.
 10. Gao, W.; Zhang, Y.; Ramanujan, D.; Ramani, K.; Chen, Y.; Williams, C.B.; Wang, C. C. L.; Shin, T. C.; Zhang, S.; Zavattieri, P. D. The Status, Challenges, and Future of Additive Manufacturing in Engineering Comput. *Aided Des.* **2015**, 69, 65-89.
 11. Zhang, Z.; Deng, J.; Li, X.; Yang, Z.; He, S.; Chen, X.; Guan, G.; Ren, J.; Peng, H. Superelastic SCs with High Performances During Stretching. *Adv. Mater.* **2015**, 27, 356-362.
 12. Li, B.; Zhang, S.; Zhang, L.; Gao, Y.; Xuan, F. Train Sensing Behavior of FDM 3D Printed Carbon Black Filled TPU with Periodic Configurations and Flexible Substrates. *J. Manuf. Process.* **2022**, 74, 283-295.
 13. Christ, J. F.; Aliheidari, N.; Ameli, A.; Tschke, P.; 3D Printed Highly Elastic Strain Sensors of Multi-walled Carbon Nanotube/thermoplastic Polyurethane Nanocomposites. *Mater. Des.* **2017**, 131, 394-401.
 14. Chen, Y.; Li, Y.; Xu, D.; Zhai, W. Fabrication of Stretchable Flexible Conductive Thermoplastic Polyurethane/graphene Composites Via Foaming, *RSC Adv.* **2015**, 5, 82034-82041.
 15. Xiang, D.; Zhang, X.; Li, Y.; Harkin-Jones, E.; Zheng, Y.; Wang, L. Enhanced Performance of 3D Printed Highly Elastic Strain Sensors of Carbon Nanotube/thermoplastic Polyurethane Nanocomposites Via Non-covalent Interactions. *Composites*, **2019**, 176, 107250.
 16. Zheng, Y.; Li, Y.; Li, Z.; Wang, Y.; Dai, K.; Zheng, G.; The Effect of Filler Dimensionality on the Electromechanical Performance of Polydimethylsiloxane Based Conductive Nanocomposites for Flexible Strain Sensors. *Compos. Sci. Technol.* **2017**, 139, 64-73.
 17. Sultan, A.; Ahmad, S.; Anwer, T.; Mohammad, F. Binary Doped Polypyrrole and Polypyrrole/boron Nitride Nanocomposites: Preparation, Characterization and Application in Detection of Liquefied Petroleum Gas Leaks, *RSC Adv.* **2015**, 5, 105980-105991.
 18. Huang, Y.; Li, H.; Wang, Z.; Zhu, M.; Pei, Z.; Xue, Q.; Huang, Y.; Zhi, C.; Nanostructured Polypyrrole as a Flexible Electrode Material of SC, *Nano Energy*. **2016**, 22, 422-438.
 19. Song, Y.; Shang, M.; Li, J.; Su, Y. Continuous and Controllable Synthesis of MnO₂/PPy Composites with Core-shell Structures for SCs, *J. Chem. Eng.* **2021**, 405, 127059.
 20. Shen, M.; Chen, L.; Chen, Y.; Li, W.; Zheng, R.; Lin, Y.; Han, D. Construction of CuO/PPy Heterojunction Nanowire Arrays on Copper Foam as Integrated Binder-free Electrode Material for High-performance SC, *J. Electroanal. Chem.* **2021**, 891, 115272.
 21. Yin, Z.; Fan, W.; Li, J.; Guan, L.; Zheng, Q. Shell Structure Control of PPy-Modified CuO Composite Nanoleaves for Lithium Batteries with Improved Cyclic Performance, *ACS Sustainable Chem. Eng.* **2015**, 3, 507-517.
 22. Karthick, S.; Susmisha, A.; Haribabu, K. Performance of Tungsten Oxide/polypyrrole Composite as Cathode Catalyst in Single Chamber Microbial Fuel Cell, *J. Environ. Chem. Eng.* **2020**, 8, 104520.
 23. Sivakkumar, S. R.; Ko, J. M.; Kim, D. Y.; Kim, B. C.; Wallace, G. G. Performance Evaluation of CNT/polypyrrole/MnO₂ Composite Electrodes for Electrochemical Capacitors. *Electrochim. Acta.* **2007**, 52, 7377-7385.
 24. Huang, M.; Li, F.; Zhang, X. Y.; Gao, X. Hierarchical NiO Nanoflake Coated CuO Flower Core-shell Nanostructures for SC, *Ceramics. Int.* **2014**, 40, 5533-5538.
 25. Kim, J. Y.; Selvam, S.; Yim, H. J. Preparation of Porous TPU-PPy Flexible Composite Using 3D Printer and Its Application as Electrode Scaffold for Energy Storage Devices, *Polym. Korea*, **2022**, 46, 389-396.
 26. Kim, J. Y.; Kim, -H, D.; Choi, S. J.; Yim, H. J. A Multi-functional Ammonia Gas and Strain Sensor with 3D-printed Thermoplastic Polyurethane-polypyrrole Composites. *Polymer*. **2022**, 240, 124490.
 27. Park, D.; Park, K. Y.; Selvam, S.; Yim, H. J. Tyrene-based Ternary Composite Elastomers Functionalized with Graphene Oxide-polypyrrole Under Iron(III)-alkyl Benzenesulfonate Oxidants for SC Integrated Strain Sensor System. *J. Energy. Storage*, **2022**, 51, 104543.
 28. Yan, L.; Xiong, T.; Zhang, Z.; Yang, H.; Zhang, X.; He, Y.; Bian, J.; Lin, H.; Chen, D. Facile Preparation of TPU Conductive Nanocomposites Containing Polypyrrole-coated Multi-walled Carbon Nanotubes for a Rapid and Selective Response in Volatile Organic Compounds Applications. *Compos. A: Appl. Sci.* **2022**, 157, 106913.
 29. Bertolini, C. M.; Zamperlin, N.; Barra, G. M. O.; Pegoretti, A. Development of Poly(vinylidene fluoride)/thermoplastic Polyurethane/carbon Black-polypyrrole Composites with Enhanced Piezoelectric Properties. *SPE Polymers.* **2023**, 4, 143-155.
 30. Mohammad, S. D.; Mostafa, Z. M. Experimental Study of Water-based CuO Nanofluid Flow in Heat Pipe Solar Collector, *J. Therm. Anal. Calorim.* **2019**, 137, 2061-2072.
 31. Ruxangul, J.; Li, Z.; Minchao, W.; Zhao, Q.; Abdiryim, T. Synthesis of Poly(3,4-propylenedioxythiophene)/MnO₂ Composites and Their Applications in the Adsorptive Removal of Methylene Blue, *Prog. Nat. Sci.; Mater. Int.* **2016**, 26, 32-40.
 32. Kim, J. Y.; Choi, S. J.; Yim, H. J. Effects of Infill Patterns on Resistance-dependent Strain and Ammonia Gas Sensing Behaviors of 3D-printed Thermoplastic Polyurethane Modified with Polypyrrole. *J. Mater. Chem. C*, **2022**, 10, 6687.
 33. Rakhi, B. R.; Alhebshi, A. N.; Anjum, D. H.; Alshreef, H. N.; Nanostructured Cobalt Sulfide-on-fiber with Tunable Morphology as Electrodes for Asymmetric Hybrid SCs, *J. Mater. Chem. A*,

- 2014**, 2, 16190-16198.
34. Xu, J.; Wang, D.; Yuan, Y.; Wei, W.; Duan, L.; Wang, L.; Bao, H.; Xu, W. Polypyrrole/reduced Graphene Oxide Coated Fabric Electrodes for Supercapacitor Application. *Organic Electronics*, **2015**, 24, 153-159.
35. Kakani, V.; Ramesh, S.; Lee, H.; Kim, H. Hydrothermal Synthesis of CuO@MnO₂ on Nitrogen-doped Multiwalled Carbon Nanotube Composite Electrodes for SC Applications. *Sci. Rep.* **2022**, 12, 12951.
36. Palem, R. R.; Ramesh, S.; Bathula C.; Kim, H. J.; Lee, H. S.; Kakani, V.; Saratale, C. D.; Yadav, H. M. Enhanced Supercapacitive Behavior by CuO@MnO₂/Carboxymethyl Cellulose Composites. *Ceramics Intl.* **2021**, 47, 26738-26747.
37. Yang, J.; Cao, J.; Peng, Y.; Bisset, M.; Kinloch, I. A.; Dryfe, R. A. W. Unlocking the Energy Storage Potential of Polypyrrole Via Electrochemical Graphene Oxide for High Performance Zinc-ion Hybrid Supercapacitors. *J. Power. Sources*, **2021**, 516, 230663.
38. Gunawardana, M. K.; Disanayaka, H. N.; Fernando, M. S.; de Silva, K. M. N.; de Silva, R. M. Development of Graphene Oxide-based Polypyrrole Nanocomposite for Effective Removal of Anionic and Cationic Dyes from Water. *Results Chem*, **2023**, 6, 101079.
39. Deka, B. K.; Hazarika, A.; Kang, G.-H.; Hwang, Y. J.; Jaiswal, A. P.; Kim, D. C.; Park, Y. B.; Park, H. W. 3D-Printed Structural Supercapacitor with MXene-N@Zn-Co Selenide Nanowire Based Woven Carbon Fiber Electrodes. *ACS Energy Lett.* **2023**, 8, 963-971.
40. Idrees, M.; Ahmed, S.; Mohammed, Z.; Korivi, S. N.; Rangari, V. 3D Printed Supercapacitor Using Porous Carbon Derived from Packaging Waste. *Additi Manuf*, **2020**, 36, 101525.
41. Lin, D.; Swetha, C.; Jean, B. F.; Xinzhe, X.; Anica, P.; Emma, C.; Marcus, A. W. 3D-Printed Graded Electrode with Ultrahigh MnO₂ Loading for Non-Aqueous Electrochemical Energy Storage. *Adv. Energy Mater.* **2023**, 13, 2300408.
42. Zhu, G.; Hou, Y.; Lu, J.; Zhang, Z.; Baig, M. M.; Muhammad, Z. K.; Muhammad, A. A.; Dong, S.; Liu, P.; Ge, X.; Zhang, Y. MXene Decorated 3D-printed Carbon Black-based Electrodes for Solid-state Micro-supercapacitors. *J. Mater. Chem. A*, **2023**, 11, 25422.
43. Ghosh, K.; Pumera, M. Free-standing Electrochemically Coated MoS_x Based 3D-printed Nanocarbon Electrode for Solid-state Supercapacitor Application. *Nanoscale*, **2021**, 13, 5744-5756.
44. Lee, J.; Jeong, H.; Lavall, R. L.; Busnaina, A.; Kim, Y.; Jung, Y. J.; Lee, H. Y. Polypyrrole Films with Micro/Nanosphere Shapes for Electrodes of High-performance Supercapacitors. *ACS Appl. Mater. Interfaces*. **2017**, 9, 38, 33203-33211.
45. Nodora, K. M.; Yim, J. H. Study of Growth Mechanism of Conductive Free-standing Films on a Vapor/Water Interface via Gas Phase Polymerization. *Polym. Korea*, **2021**, 45, 267-274.
46. Jeong, Y.; Moon, B. C.; Kim, Y. Preparation and Characterization of Conducting Polymer Nanocomposites Including Graphene Oxide via In-situ Chemical Polymerization. *Polym. Korea*, **2014**, 38, 180-187.

Publisher's Note The Polymer Society of Korea remains neutral with regard to jurisdictional claims in published articles and institutional affiliations.